

Drive-by-wire Vehicle Stabilization and Yaw Regulation: a Hybrid Model Predictive Control Design

D. Bernardini[†], S. Di Cairano[‡], A. Bemporad[†], H.E. Tseng[‡]

Abstract—Electronic Stability Control (ESC) and Active Front Steering (AFS) have been introduced in production vehicles in recent years, due to improved vehicle maneuverability and the effects in reducing single vehicle accident. We propose a hybrid Model Predictive Control (MPC) design for coordinated control of AFS and ESC. By formulating the vehicle dynamics with respect to the front and rear tire slip angles and by approximating the tire-force characteristics by piecewise affine functions, the vehicle dynamics are formulated as a linear hybrid dynamical system. This model is used to design a hybrid model predictive controller. The proposed model formulation allows one to visually analyze the stability region of the closed-loop system and to assess the stabilizing capability of the hybrid MPC controller. Simulations of the controller in closed-loop with an accurate nonlinear model are presented.

I. INTRODUCTION

Electronic Stability Control (ESC) [1] and Active Front Steering (AFS) [2] have been introduced to many production vehicles in recent years, due to their capability of reducing single vehicle accidents. Both have drawn a lot of attentions in research literature [1]–[4].

Since both AFS and ESC are driver-assist systems that improve vehicle yaw and lateral stability, it is innate for one to ask how the two can be best combined together in system design, or how the actuations of the two systems, if individually designed, would be best arbitrated. One concept that has been demonstrated with some successful results in double lane change maneuvers [5] is to decouple the two systems. A different approach is to utilize linear MIMO control synthesis by applying μ -synthesis to a transformed model of the vehicle, and by optimizing the control objective under structured model uncertainties [3].

In this paper, we propose a hybrid Model Predictive Control (MPC) design for the coordinated control of the two actuators. The major advantage of MPC is the capability of handling in a single framework multiple inputs and outputs, constraints on inputs, states, and outputs, and optimization with respect to a predefined performance criterion [6].

In recent years, MPC has been successfully applied to problems related to vehicle dynamics and handling [7], [8]. Recently, in [8] a nonlinear MPC approach was proposed for coordination of active steering and braking in an autonomous vehicle navigating along a known trajectory. Due to the computational burden of nonlinear MPC, the same authors

have proposed a linear time varying formulation of the MPC problem, which can be solved as a quadratic program. This reduces dramatically the amount of time required by the optimization algorithm, so that the controller can run at a higher rate and an improved performance is achieved. However, this approach still requires the optimization algorithm to run on line, therefore setting high requirements for CPU power and memory of the vehicle ECU, as well as the need to execute the optimization software in the ECU.

In this paper we consider a similar yet different problem in which the control objective is to force the vehicle yaw rate to track a given reference. Such a reference, not known in advance, is computed from the position of the steering wheel as actuated by a human driver, and from the current vehicle velocity. Hence, the steering wheel works as a reference generator, but it is the controller that physically actuates at the same time the steering and the differential braking system, resulting in a drive-by-wire architecture.

In Section II we formulate the vehicle dynamics using the front and rear tire slip angles as the states, and the vehicle yaw rate as the output. By assuming a constant longitudinal velocity and approximating the functions that relate the tire force to the tire slip angles by a piecewise affine maps, the vehicle dynamics are reformulated as a linear hybrid system in piecewise affine (PWA) form. By transforming the PWA model in an equivalent mixed-logical dynamical (MLD) system [9], the obtained vehicle dynamics formulation is used as a prediction model in a hybrid model predictive control setup [10], in Section III. After adding integral action and constraints on system states, inputs and outputs, the behavior of the nonlinear vehicle dynamics in closed-loop with the hybrid MPC controller is analyzed in simulation in Section IV. By simply looking at the phase-plane plots of the tire slip angle trajectories for the open-loop and closed-loop dynamics, one can directly visualize the stable regions of the vehicle dynamics. Controller robustness is tested in simulation with respect to variations of model parameters, namely the road friction coefficient and the vehicle longitudinal velocity. The introduced integral action, besides providing zero steady-state tracking errors, guarantees a remarkable degree of robustness with respect to parameters variations.

II. VEHICLE MODEL

In this paper we consider the control of the passenger vehicle dynamics, where two inputs are available for the controller, the front steering angle, and the yaw moment generated by differential braking. The steering wheel controlled

[†] D. Bernardini and A. Bemporad are with the Department of Information Engineering, University of Siena, Italy, {bernardini,bemporad}@dii.unisi.it.

[‡] S. Di Cairano and H.E. Tseng are with Powertrain Control R&A, Ford Motor Company, Dearborn, MI, {sdicaira,htseng}@ford.com.

by the driver is decoupled from the wheels. The steering wheel position is read from a sensor and, combined with information regarding vehicle velocity, is converted into a reference yaw rate. The purpose of the controller is to track the above indicated reference, hence providing the driver with the desired yaw rate.

For modelling vehicle dynamics in high speed turns¹ a bicycle model of the vehicle is appropriate [11], which is presented in Figure 1. We consider a reference frame that

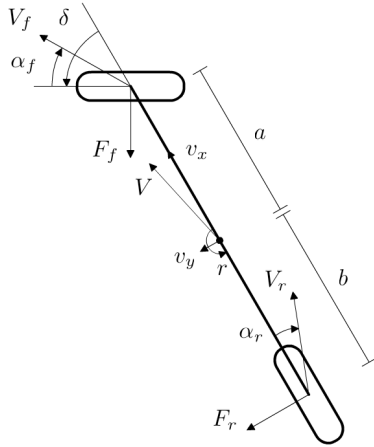


Fig. 1. Schematics of the bicycle model of the vehicle.

moves with the vehicle. We set the reference frame origin in the vehicle center of mass, where the x -axis is along the longitudinal vehicle direction, the y -axis is transversal to the vehicle direction, and the z -axis is pointing upwards, so that angles increase counterclockwise. The tire slip angle is the angle between the tire direction and the velocity vector at the tire.² Hence, in the bicycle model, two tire slip angles are defined, α_f [rad] and α_r [rad], at the front and at the rear tires, respectively. Note that according to the used reference frame the front and rear tire slip angles in Figure 1 are negative.

Since the longitudinal component of the velocity at the wheels is the same than the one at the center of mass v_x [m/s], and the lateral velocity is computed by adding to the lateral velocity at the center of mass v_y [m/s] the contribution due to the rotation, the tire slip angles can be expressed as

$$\tan(\alpha_f + \delta) = \frac{v_y + ar}{v_x}, \quad (1a)$$

$$\tan \alpha_r = \frac{v_y - br}{v_x}, \quad (1b)$$

where a [m] and b [m] are the distances of the front and rear wheel axes from the vehicle center of mass, respectively, δ [rad] is the steering angle, and r [rad/s] is the vehicle

¹Turns that are performed in normal “on-road” driving are referred to as *high speed* turns. *Low speed* turns are those turn manoeuvres that occurs for instance when parking and merging [11].

²In some works the tire slip angles are defined with the opposite sign with respect to the one used here. This is obviously just a matter of convention and does not affect the validity of the approach and the results presented in this paper.

yaw rate. In this paper we will avoid to explicitly show the dependance in time of the variables, when not needed. The front and rear tire forces F_f [N], F_r [N], respectively, are nonlinear functions of the tire slip angles α_f , α_r and of the longitudinal slip³ $s \in [0, 1]$. We use a model of the tire forces which, for a constant longitudinal slip s , is piecewise linear

$$F_f(\alpha_f) = \begin{cases} -c_f \alpha_f & \text{if } -\hat{p}_f \leq \alpha_f \leq \hat{p}_f, \\ -(d_f \alpha_f + e_f) & \text{if } \alpha_f > \hat{p}_f, \end{cases} \quad (2a)$$

$$F_r(\alpha_r) = \begin{cases} -c_r \alpha_r & \text{if } -\hat{p}_r \leq \alpha_r \leq \hat{p}_r, \\ -(d_r \alpha_r + e_r) & \text{if } \alpha_r > \hat{p}_r, \end{cases} \quad (2b)$$

where $c_{f,r} = \tilde{c}_{f,r}(1 - s)$, $d_{f,r} = \tilde{d}_{f,r}(1 - s)$, $e_{f,r} = \hat{p}_{f,r}(\tilde{c}_{f,r} - \tilde{d}_{f,r})$ are empirically identified, and all have measurement unit [N/rad]. The complete models of the tire force-slip angle relations will require additional affine equations for the cases $\alpha_f < -\hat{p}_f$, $\alpha_r < -\hat{p}_r$. However, model (2) is appropriate for clockwise turns, while counterclockwise turns can be handled by opportunely inverting the sign of the inputs and of the system variables, and recasting the trajectory of a counterclockwise turn as a clockwise one. The force equation (2) is simplified in order to reduce the complexity of the dynamical model.

Since the tire slip angles are small for high speed turns [11] we can approximate $\tan \alpha \simeq \alpha$, hence getting

$$\alpha_f = \frac{v_y + ar}{v_x} - \delta, \quad (3a)$$

$$\alpha_r = \frac{v_y - br}{v_x}. \quad (3b)$$

Assume now that during the turning manoeuvre the longitudinal velocity v_x is constant. Then, by differentiating (3), we obtain

$$\dot{\alpha}_f = \frac{\dot{v}_y + ar}{v_x} - \dot{\delta}, \quad (4a)$$

$$\dot{\alpha}_r = \frac{\dot{v}_y - br}{v_x}. \quad (4b)$$

From (3), $\alpha_f - \alpha_r = \frac{v_y + ar}{v_x} - \delta - \frac{v_y - br}{v_x}$, so that a relation between the tire slip angles α_f , α_r and the vehicle yaw rate r is obtained,

$$r = \frac{v_x}{a + b}(\alpha_f - \alpha_r + \delta). \quad (5)$$

When the longitudinal velocity v_x is constant, the vehicle acceleration can be decomposed into the acceleration related to as if the vehicle frame were rotating with constant yaw rate r , and the lateral acceleration at the center of mass. Since the only acting forces on the vehicle are the forces at the front and rear tires F_f and F_r , respectively, we have

$$\dot{v}_y = \frac{F_f \cos \delta + F_r}{m} - r v_x. \quad (6)$$

³The longitudinal slip is defined as the normalized difference between the wheel axle velocity and the velocity at the wheel. The condition $s = 0$ indicates the two to be equal, which means perfect (ideal) adhesion to the road surface.

TABLE I
NUMERICAL VALUES OF PARAMETERS

Parameter	Value	Parameter	Value
\hat{p}_f	0.101 rad	\hat{p}_r	0.057 rad
c_f	$9.059 \cdot 10^4$ N/rad	c_r	$1.651 \cdot 10^5$ N/rad
d_f	$-9.059 \cdot 10^3$ N/rad	d_r	$-1.651 \cdot 10^4$ N/rad
e_f	$1.005 \cdot 10^4$ N/rad	e_r	$1.033 \cdot 10^4$ N/rad
a	1.47 m	b	1.43 m
m	1891 kg	I_z	3213 kgm^2
v_x	20 m/s	s	0

The yaw acceleration is computed from the torques acting on the vehicle

$$\dot{r} = \frac{aF_f \cos \delta - bF_r + Y}{I_z}, \quad (7)$$

where I_z [kg m²] is the vehicle inertia computed with respect to the center of mass, and Y [Nm] is the yaw moment applied by differential braking. For small steering angles δ , $\cos \delta \simeq 1$, hence substituting (5), (6) and (7) into (4), and neglecting the (typically small) contribution of $\dot{\delta}$ we obtain

$$\begin{aligned} \dot{\alpha}_f &= \frac{F_f + F_r}{mv_x} - \frac{v_x}{a+b}(\alpha_f - \alpha_r + \delta) + \frac{a}{v_x I_z}(aF_f - bF_r + Y), \\ \dot{\alpha}_r &= \frac{F_f + F_r}{mv_x} - \frac{v_x}{a+b}(\alpha_f - \alpha_r + \delta) - \frac{b}{v_x I_z}(aF_f - bF_r + Y). \end{aligned} \quad (8)$$

The vehicle dynamics model defined by Equations (2), (5), (8) is a second order system with states α_f, α_r , inputs δ, Y , and output r . The numerical values of the parameters for the vehicle model considered in this paper are reported in Table I.

A. Piecewise affine model

In the model defined by (2), (5), (8), the only nonlinearities are due to the tire force - tire slip angle relation (2) which, for constant longitudinal slip s , are piecewise affine functions. Thus, the overall dynamics can be formulated as a PWA system, which is a suitable prediction model for a hybrid model predictive control strategy.

Let $x = [\alpha_f \ \alpha_r]'$ and $u = [Y \ \delta]'$ be the state and the input of the system. In order to represent the nonlinearities in (2), we define two Boolean variables $\gamma_f, \gamma_r \in \{0, 1\}$ by the switching conditions

$$\gamma_f = 0 \iff \alpha_f \leq \hat{p}_f, \quad (9a)$$

$$\gamma_r = 0 \iff \alpha_r \leq \hat{p}_r. \quad (9b)$$

Thus, the piecewise affine dynamics are

$$\dot{x}(t) = A_{ij}^c x(t) + B_{ij}^c u(t) + f_{ij}^c \quad \text{if } (\gamma_f = i \wedge \gamma_r = j), \quad (10)$$

$i, j \in \{0, 1\}$, where matrices A_{ij}^c, B_{ij}^c , and vectors f_{ij}^c are obtained from (8) and (2) for the angles α_f, α_r in the region where $\gamma_f = i, \gamma_r = j$. The system matrix A_{ij}^c in (10) is stable only in the case $i = 0, j = 0$, as it is obvious from the dynamics of the forces acting on the tires.

The piecewise affine dynamics (10) are discretized in time using a sampling period $T_s = 100\text{ms}$, resulting in the

following discrete-time PWA model with four regions

$$x(k+1) = A_i x(k) + B_i u(k) + f_i, \quad (11a)$$

$$i \in \{1, \dots, 4\} \quad : \quad H_i x(k) \leq K_i, \quad (11b)$$

where A_i, B_i, f_i directly follow from (10), while H_i, K_i are the inequalities describing the polyhedral regions associated to different linear expressions in force equations (2), as defined in the right hand side of (9). The discrete-time PWA model (11) can be formulated as an MLD system [9], [10] and used in a hybrid MPC control algorithm.

III. HYBRID MPC DESIGN

In this section, we propose a formulation of the feedback control problem within a hybrid system framework. Hybrid systems provide a unified framework for describing processes that evolve according to continuous dynamics, discrete dynamics, and logic rules [12], [13]. The interest in hybrid systems is mainly motivated by the large variety of practical situations where physical processes interact with digital controllers, as for instance in embedded systems. Several modeling formalisms have been developed to describe hybrid systems [9], including PWA and MLD systems. The language HYSDEL (HYbrid Systems DESCRIPTION Language) was developed in [14] to obtain MLD models from a high level textual description of the hybrid dynamics. HYSDEL models are used in the Hybrid Toolbox for Matlab [15] for modeling, simulating, and verifying the safety properties of hybrid systems and for designing and prototyping hybrid MPC controllers.

Hybrid model predictive control has been recently applied to problems in automotive systems [7], [16], [17]. In the MPC strategy, at each sampling instant a finite horizon open-loop optimal control problem is solved, by using the current state as the initial condition. The optimization results in an optimal control sequence, where only the first element is actually applied to the system, while the remaining ones are simply discarded. At the next sampling instant a new optimization problem is solved, where the updated information on the system, for instance obtained from new measurements, is exploited, thereby introducing a feedback mechanism.

A. Reference generation

In our framework, the purpose of the controller is to stabilize system (11) at the equilibrium obtained from the time-varying driver's steering command $\hat{\delta}(k)$, read by an on-board sensor, while minimizing the use of the brake actuator (i.e., $\hat{Y}(k) = 0$, for all k). By computing the equilibrium state of (10) in the linear region (i.e., $\gamma_f = \gamma_r = 0$), with $\delta = \hat{\delta}, Y = \hat{Y}$, we obtain the equilibrium condition

$$\hat{\alpha}_r(k) = \hat{\alpha}_f(k) \frac{ac_f}{bc_r}. \quad (12)$$

Using (5), (10), and (12), we define the set-points of our control problem as follows

$$\hat{\alpha}_f = \frac{m\tilde{v}_x^2 bc_r \hat{\delta}}{m\tilde{v}_x^2 (ac_f - bc_r) - c_f c_r (a+b)^2}, \quad (13a)$$

$$\hat{\alpha}_r = \hat{\alpha}_f \frac{ac_f}{bc_r}, \quad (13b)$$

$$\hat{r} = \frac{\tilde{v}_x}{a+b} (\hat{\alpha}_f - \hat{\alpha}_r + \hat{\delta}), \quad (13c)$$

where time dependency is omitted for brevity, and \tilde{v}_x is the current available measurement of the real longitudinal velocity of the vehicle. In general, the value of \tilde{v}_x will be different from v_x , the longitudinal velocity used in the MPC prediction model.

B. Hybrid prediction model

The main goal of the control action is to track the yaw rate set-point \hat{r} , which retains information about the driver's desired trajectory, by manipulating the steering angle δ and the vehicle's yaw moment Y . According to model (5), r is the output of our system. In order to reject constant disturbances, reduce the effect of model inaccuracies, and ensure a zero tracking error in steady state, we add integral action on the yaw rate tracking. In details, we extend system (11) by

$$I_r(k+1) = I_r(k) + r(k) - r_s(k), \quad (14a)$$

$$r_s(k+1) = r_s(k), \quad (14b)$$

where I_r is the cumulated sum of yaw rate tracking errors, and r_s is the yaw rate set-point, which is assumed to be constant along the prediction horizon, since preview information on the human driver action is not available. Then, by defining $z = [\alpha_f \ \alpha_r \ I_r \ r_s]'$, $u = [Y \ \delta]'$, $y = r$, the hybrid dynamical model used for prediction in our controller is

$$\begin{aligned} z(k+1) &= \tilde{A}_i z(k) + \tilde{B}_i u(k) + \tilde{f}_i, \\ y(k) &= \tilde{C}_i z(k) + \tilde{D}_i u(k), \\ i &\in \{1, \dots, 4\} : \tilde{H}_i z(k) \leq \tilde{K}_i, \end{aligned} \quad (15)$$

where

$$\begin{aligned} \tilde{A}_i &= \begin{bmatrix} A_i & 0 & 0 \\ \frac{v_x}{a+b} & \frac{-v_x}{a+b} & 1 & -1 \\ 0 & 0 & 0 & 1 \end{bmatrix}, \quad \tilde{B}_i = \begin{bmatrix} B_i \\ 0 & \frac{v_x}{a+b} \\ 0 & 0 \end{bmatrix}, \quad \tilde{f}_i = \begin{bmatrix} f_i \\ 0 \\ 0 \end{bmatrix}, \\ \tilde{C}_i &= \begin{bmatrix} \frac{v_x}{a+b} & \frac{-v_x}{a+b} & 0 & 0 \end{bmatrix}, \quad \tilde{D}_i = \begin{bmatrix} 0 & \frac{v_x}{a+b} \end{bmatrix}, \\ \tilde{H}_i &= \begin{bmatrix} H_i & 0 & 0 \end{bmatrix}, \quad \tilde{K}_i = K_i. \end{aligned}$$

C. Constraints

The control action is subject to the following constraints, related to physical limits of the actuators,

$$\begin{aligned} |[u]_1(k)| &\leq 1000 \text{ [Nm]}, \\ |[u]_2(k)| &\leq 0.35 \text{ [rad]}, \end{aligned} \quad (16)$$

where for a vector a , $[a]_i$ indicates the i -th component of the vector. Moreover, as mentioned in Section II-A, for simplicity we restrict to consider a subset of the tire slip angles space, by imposing

$$\begin{aligned} [z]_1(k) &\geq -\hat{p}_f, \\ [z]_2(k) &\geq -\hat{p}_r. \end{aligned} \quad (17)$$

D. Finite horizon optimal control problem

At any time step k , the optimal control problem to be solved is formulated as

$$\begin{aligned} \min_{\mathbf{u}_k} \quad & \sum_{j=0}^{N-1} \left\{ (z_{k+j|k} - \hat{z})' Q_z (z_{k+j|k} - \hat{z}) \right. \\ & + (y_{k+j|k} - \hat{y})' Q_y (y_{k+j|k} - \hat{y}) \\ & \left. + (u_{k+j|k} - \hat{u})' Q_u (u_{k+j|k} - \hat{u}) \right\} \end{aligned} \quad (18a)$$

$$\text{s.t.} \quad (15), (16), (17), \quad (18b)$$

$$z_{k|k} = z(k), \quad (18c)$$

where N is the control horizon, $\mathbf{u}_k = (u_{k|k}, \dots, u_{k+N-1|k})$ is the sequence of control input that is the optimization problem decision variable, $z(k)$ and $y(k)$ are the measured state and output of system (15) at time k , $\hat{z} = [\hat{\alpha}_f \ \hat{\alpha}_r \ 0 \ 0]'$, $\hat{y} = \hat{r}$, $\hat{u} = [\hat{Y} \ \hat{\delta}]'$ are the set-points, which are recomputed at every sample time from the measured values of $\hat{\delta}$ and \tilde{v}_x , and Q_z , Q_u , Q_y are positive semidefinite weight matrices of appropriate dimensions. Using HYSDEL and the Hybrid Toolbox, problem (18) is translated into a mixed-integer quadratic program (MIQP), i.e., into the minimization of a quadratic cost function subject to linear constraints, where some of the variables are constrained to be integer (binary, in our specific case). According to the receding horizon mechanism, the first move $u_{k|k}^*$ of the optimizer \mathbf{u}_k^* of (18) is used as control input at time k , i.e.,

$$u(k) = u_{k|k}^*. \quad (19)$$

IV. SIMULATION EXAMPLES

The proposed control scheme was tested in simulation on a nonlinear vehicle model, which takes into account the dynamics of yaw rate, longitudinal and lateral dynamics, and steering actuation dynamics. A detailed description of this nonlinear simulation model is beyond the scope of this paper and it is omitted, also for brevity. The control horizon used in simulation is $N = 3$, which after a calibration process resulted in a good performance and an acceptable computational burden. The weight matrices are $Q_z = \begin{bmatrix} .1 & 0 & 0 & 0 \\ 0 & .1 & 0 & 0 \\ 0 & 0 & 1 & 0 \\ 0 & 0 & 0 & 0 \end{bmatrix}$, $Q_u = \begin{bmatrix} 1 & 0 \\ 0 & 1 \end{bmatrix}$, $Q_y = 1$. In the following, the driver's steering command $\hat{\delta}$ has been considered constant over the whole simulation interval.

A first set of tests is carried out in nominal conditions, i.e., with the parameters in the nonlinear simulation model having the same numerical value than the parameters used to build the control-oriented hybrid prediction model (11). Even under nominal conditions the control strategy has to cope with the errors due to linearization of the nonlinear dynamics (e.g., in (1)), which affect the simulated trajectories. We have analyzed the ability of the vehicle to recover from poor initial conditions on the tire slip angles $(\alpha_f(0), \alpha_r(0)) = (0.05, 0.15)$, for which the corresponding matrix of the PWA system (10) is unstable. Figure 2 shows a comparison between closed-loop and open-loop performance in terms of

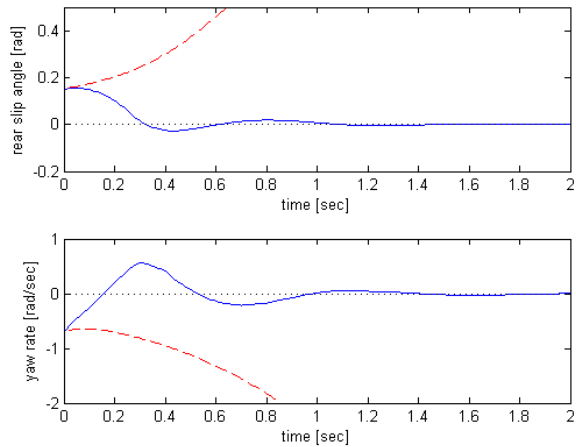


Fig. 2. Closed-loop (blue line), open-loop (red dashed line), and set-point (black dotted line) trajectories of rear tire slip angle α_r and yaw rate r , with $\alpha_f(0) = 0.05$, $\alpha_r(0) = 0.15$, and $\delta = 0$.

rear tire slip angle α_r and yaw rate r trajectories.⁴ While in open-loop the vehicle is led into spinning, in the closed-loop simulation the controller achieves a fast stabilization and a correct tracking of the desired yaw rate. Stability of the vehicle behavior at various initial tire slip angles is illustrated in Figure 3, where one can see that the control action increases the stable region despite the destabilizing effect introduced by the integral action, which is in fact an additional non asymptotically stable dynamics.

Then, we tested the robustness of the control action with respect to mismatches between the modeled parameters values and their actual value in simulation. Figures 4, 5 illustrate the closed-loop behavior in the case of different values of the real longitudinal velocity \tilde{v}_x , and the related optimal inputs trajectories. The values of \tilde{v}_x are still assumed to be measured, so that the set-points can be computed properly. Again, the plots show the stability of the closed-loop and a fast tracking response. Note also that at steady state the value of the differential braking actuator is different from 0, and depends on the type of disturbance. This indicates that the controller selects this actuator to counteract the parameter variations.

Finally, we analyzed the behavior of the controlled vehicle in a turning manoeuvre under perturbed initial conditions on the tire slip angles and a non-ideal longitudinal slip $s > 0$, caused for instance by slippery road surface. Yaw rate trajectories related to different values of s , plotted in Figure 6, show a good degree of robustness with respect to model mismatches.

The simulations have been executed on a Macbook 2.4GHz with Matlab 7.6 and CPLEX 9.0. We obtained an average computation time of 17 ms per time step (63 ms in the worst case). This encourages the viability of the proposed approach for experimental tests, although on-line

⁴Front tire slip angle trajectories are analogous and are omitted for lack of space.

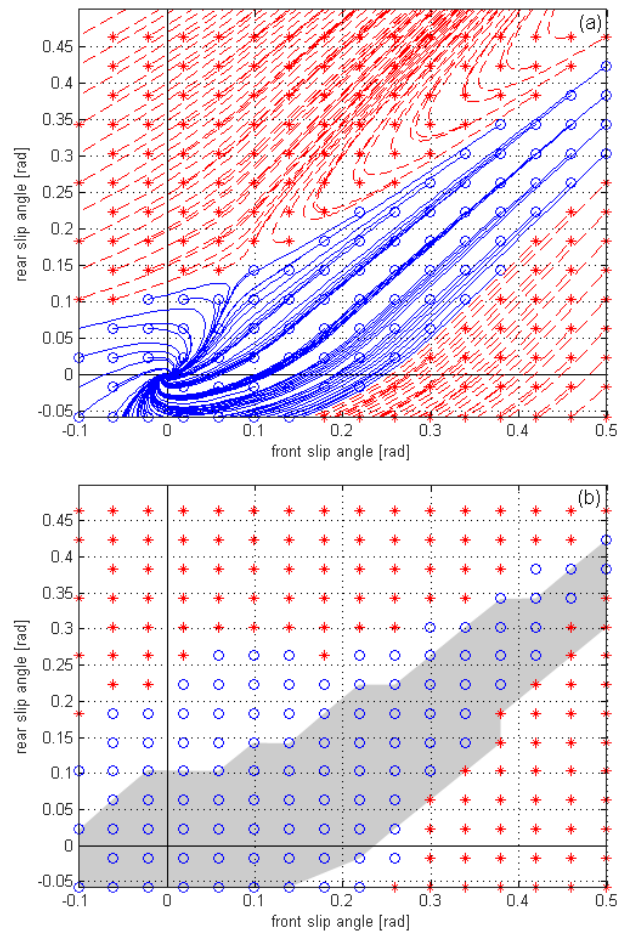


Fig. 3. Stability region of the vehicle behavior in (a) open-loop, and (b) closed-loop, at various initial tire slip angles. Blue circles and red stars denote stable and unstable behavior, respectively. In (a) tire slip angles trajectories in time are shown. In (b) the set of open-loop stable initial conditions is plotted in grey for comparison.

optimization should be avoided in the implementation in standard automotive ECU. By employing multiparametric programming techniques, we can solve the MIQP control problem off-line for all state vectors and references within a given range. The state-times-reference space is subdivided into polyhedral regions. In each of these regions, the control law is defined by a (possibly) different piecewise affine function of the state and the reference. In this way, the control input is computed by evaluating a PWA function with possibly overlapping partitions, see [18] for a recent survey on explicit MPC techniques.

The explicit solution of problem (18) requires a large number of regions to be stored (namely, around 5000). Our preliminary tests have shown that this number can be substantially reduced (more than halved) just by carefully selecting the operating range of the slip angles. However, an approximation might be needed to further reduce the memory occupancy requirements on the ECU. Viable approaches are either the approximation of the explicit control law by interpolation methods, or the implementation of a suboptimal switched linear MPC law, which is currently

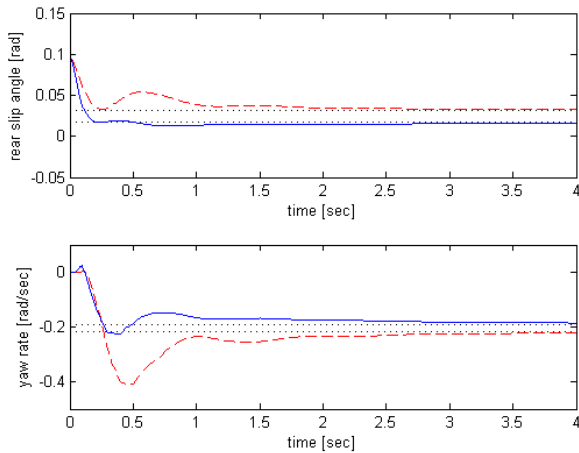


Fig. 4. Closed-loop trajectories of rear tire slip angle α_r and yaw rate r at different values of real longitudinal velocity \tilde{v}_x (blue line: $\tilde{v}_x = 15m/s$, red dashed line: $\tilde{v}_x = 25m/s$, black dotted lines: set-points), with nominal velocity $v_x = 20m/s$, $\alpha_f(0) = \alpha_r(0) = 0.1$, and $\hat{\delta} = -0.05$.

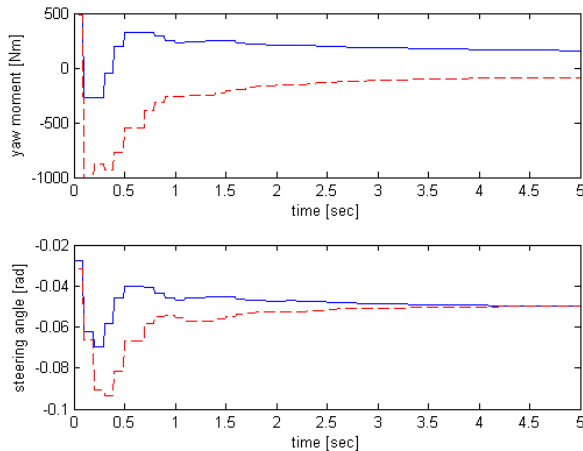


Fig. 5. Closed-loop actuation profiles of steering angle $\hat{\delta}$ and yaw moment Y at different values of real longitudinal velocity \tilde{v}_x (blue line: $\tilde{v}_x = 15m/s$, red dashed line: $\tilde{v}_x = 25m/s$), with nominal velocity $v_x = 20m/s$, $\alpha_f(0) = \alpha_r(0) = 0.1$, and $\hat{\delta} = -0.05$.

being developed.

V. CONCLUSIONS

In this paper we have proposed a hybrid model predictive control approach for coordinating the active front steering and the electronic stability control actuators. By formulating the vehicle dynamics with respect to the front and rear tire slip angles, and by approximating the tire force characteristics by piecewise affine functions, the optimization problem of the MPC controller is formulated as a mixed-integer quadratic problem. The proposed model formulation allows to visually analyze the stability region of the closed-loop dynamics. Simulations in nominal and non-nominal conditions have been shown, which suggest hybrid MPC as a promising and viable candidate for the application.

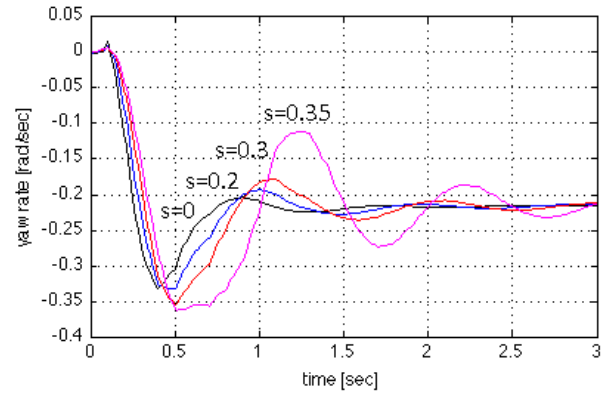


Fig. 6. Closed-loop trajectories of yaw rate r at different values of real longitudinal slip \bar{s} , with nominal value $s = 0$, $\alpha_f(0) = \alpha_r(0) = 0.1$, and $\hat{\delta} = -0.05$.

REFERENCES

- [1] K. Koibuchi, Y. Masaki, Y. Fukada, and I. Shoji, "Vehicle stability control in limit cornering by active braking," in *SAE paper*, no. 960487, 1996.
- [2] J. Ackermann, "Robust control preventing car skidding," *Control Systems Magazine*, vol. 17, no. 3, pp. 23–31, 1997.
- [3] E. Ono, K. Takanami, N. Iwama, Y. Hayashi, Y. Hirano, and Y. Satoh, "Vehicle integrated control for steering and traction systems by μ -synthesis," *Automatica*, vol. 30, no. 11, pp. 1639–1647, 1994.
- [4] E. Ono, S. Hosoe, D. Hoang, and S. Doi, "Bifurcation in vehicle dynamics and robust front wheel steering control," *IEEE Trans. Contr. Systems Technology*, vol. 6, no. 3, pp. 412–420, 1998.
- [5] D. Odenthal, T. Bunte, and J. Ackermann, "Nonlinear steering and braking control for vehicle rollover avoidance," in *Proc. European Control Conf.*, Karlsruhe, Germany, 1999.
- [6] J. Rawlings, "Tutorial overview of model predictive control," *Control Systems Magazine*, pp. 38–52, 2000.
- [7] F. Borrelli, A. Bemporad, M. Fodor, and D. Hrovat, "An MPC/hybrid system approach to traction control," *IEEE Trans. Contr. Systems Technology*, vol. 14, no. 3, pp. 541–552, 2006.
- [8] P. Falcone, F. Borrelli, J. Asgari, H. Tseng, and D. Hrovat, "Predictive active steering control for autonomous vehicle systems," *IEEE Trans. Contr. Systems Technology*, vol. 15, no. 3, pp. 566–580, 2007.
- [9] W. Heemels, B. de Schutter, and A. Bemporad, "Equivalence of hybrid dynamical models," *Automatica*, vol. 37, no. 7, pp. 1085–1091, 2001.
- [10] A. Bemporad and M. Morari, "Control of systems integrating logic, dynamics, and constraints," *Automatica*, vol. 35, no. 3, pp. 407–427, 1999.
- [11] T. Gillespie, *Fundamentals of vehicle dynamics*. Society of Automotive Engineers, Inc., 1992.
- [12] P. Antsaklis, "A brief introduction to the theory and applications of hybrid systems," *Proc. IEEE, Special Issue on Hybrid Systems: Theory and Applications*, vol. 88, no. 7, pp. 879–886, 2000.
- [13] M. Branicky, "Studies in hybrid systems: modeling, analysis, and control," Ph.D. dissertation, LIDS-TH 2304, Massachusetts Institute of Technology, Cambridge, MA, 1995.
- [14] F. Torrisi and A. Bemporad, "HYSDDEL - A tool for generating computational hybrid models," *IEEE Trans. Contr. Systems Technology*, vol. 12, no. 2, pp. 235–249, 2004.
- [15] A. Bemporad, "Hybrid toolbox - User's guide," 2003.
- [16] N. Giorgetti, A. Bemporad, H. Tseng, and D. Hrovat, "Hybrid model predictive control application towards optimal semi-active suspension," *Int. J. Control*, vol. 79, no. 5, pp. 521–533, 2006.
- [17] S. Di Cairano, A. Bemporad, I. Kolmanovsky, and D. Hrovat, "Model predictive control of magnetically actuated mass spring dampers for automotive applications," *Int. J. Control*, vol. 80, no. 11, pp. 1701–1716, 2007.
- [18] A. Alessio and A. Bemporad, "A survey on explicit model predictive control," in *Proc. Int. Workshop on Assessment and Future Directions of Nonlinear Model Predictive Control*, Pavia, Italy, 2008.